Journal of Earth Science and Engineering 2 (2012) 22-34

A Deterministic Cellular Automata Model for Simulating Rural Land Use Dynamics: A Case Study of Lake Chad Basin

Azuka Pius Ozah[1], Anthony Dami[2] and Francis Adeyinka Adesina[3]

1. Regional Centre for Training in Aerospace Surveys (RECTAS), Obafemi Awolowo University, Ile-Ife 220005, Osun State, Nigeria

2. Department of Geography, University of Maiduguri, Maiduguri 600041, Borno State, Nigeria

3. Department of Geography, Obafemi Awolowo University, Ile-Ife 220005, Osun State, Nigeria

Received: July 25, 2011 / Accepted: November 7, 2011 / Published: January 20, 2012.

Abstract: Cellular automata (CA) models (deterministic, stochastic or hybrid) have garnered tremendous popularity as spatial simulation techniques. As powerful modelling tools, they have been successfully employed in conjunction with land-use allocation and statistical simulation models to portray the dynamics and patterns of growth in such simulation contexts as population dynamics, polycentricity, urban land-use evolution, gentrification and urban sprawl. In this study, the authors present a methodological approach based on a synergistic integration of a deterministic CA model, a Markov Chains transition model and a multi-criteria land evaluation model to determine and portray the patterns and dynamics of land-use change in a rural setting. The site chosen for this study is the Lake Chad Basin, an endorheic basin supporting a population of over twenty million people living in four African countries (Chad, Cameroon, Niger and Nigeria) where the people are among Africa's most chronically vulnerable to food insecurity due to the drastic impact of natural and anthropogenic agents of ecological transformation in the basin. Using remotely sensed images captured at three different dates (1975, 1987 and 1999) in conjunction with other supporting attribute data, simulation runs were executed to predict and construct two different future scenarios (2011 and 2023) of land-use/land-cover states. Based on the numerical and graphical results of the simulation runs, Water, Wetland, Openland and Forest land-use classes were predicted to register net losses while the Road, Settlement and Farm land-use classes were predicted to register net gains in both 2011 and 2023 simulated land-use scenarios. These predictive modelling results suggest that the Lake Chad ecosystem may inexorably undergo extensive land-use/land-cover transformation in the absence of mitigating intervention measures. The study demonstrates that the proposed methodological approach of integrated rural land-use scenario building and analysis relying on the CA-based land-use simulation model is a powerful and compelling tool with significant potentials to support planning and policy for sustainable rural land development.

Key words: Cellular automata, grid cell, state transition, land-use/land-cover, transition potential model, Markov Chains model, transition rule.

1. Introduction

Issues relating to land management and land-use change in both rural and urban settings dominate the development agenda of all countries of the world and, over the years, have remained highly political and contentious. This is expected in the context in which optimal land-use planning is perceived as an indispensable factor for ensuring food security, environmental sustainability and economic development. One of the recent studies on the impact of increased pressure on land and the effects of land-use and land management practices on the dynamic character of rural ecosystems shows that a strong correlation exists between balanced, sustainable land development and, human, food and environmental security [1]. Other recent studies on land management indicate that, in many parts of the world, the rural

Corresponding author: Azuka Pius Ozah, senior lecturer, master, main research fields: 3D GIS, urban and environmental science, databases. E-mail: azukaozah@yahoo.com.

landscape is experiencing rapid land-use/land-cover (LULC) changes [2]. It is not surprising therefore that the issue of rural land use change occupies the front-burner of the development initiatives of responsible governments all over the world. The desire of planning authorities and municipal governments is to articulate policies and programmes capable of maintaining a balanced ecosystem or to mitigate or prevent, on a sustainable basis, the devastating consequences of severe land-use change when they occur. Achieving this goal requires that such authorities must adopt responsible, holistic and sustainable development strategies which must axiomatically be carried out using spatial decision support tools and methodologies.

The spatio-temporal dynamics of rural ecosystems is an invariably complex phenomenon that involves a complex nexus of interacting forces of causal agents. It has been demonstrated that, in order to disentangle the complex suite of socio-economic and bio-physical forces that influence the rate, spatial pattern and distribution of land use change and to estimate the impacts of such changes, spatially-explicit land use models are indispensable [3]. As reproducible tools, such spatial simulation models have the potential to expand the planner's knowledge domain and to support the exploration of future land use changes under different scenario conditions, thus supplementing his existing mental capabilities to analyze land use change and to make more informed decisions. Such tools can help to predict ecological responses to changing landscape heterogeneity and to gain insights into the variability of landscape patterns and processes over time.

The research on dynamic landscape modelling using spatial simulation models is quite extensive and varied [4]. These models have been successfully applied in such domains as land-use allocation and land-use planning. The most recent of these spatial simulation models are based on simulated annealing, genetic algorithms, cellular automata (CA), or agent based models. Until this recent development, spatial simulation models were exclusively based on techniques such as differential equations, partial differential equations and empirical equations. CA models (deterministic, stochastic or hybrid) have recently garnered tremendous popularity as a spatial simulation technique in a wide range of urban and rural land-use simulation and modelling domains and, as such, the vistas of research in this direction are rapidly expanding. Over the past few years, CA models have found application in spatial simulation involving a plethora of themes including, among others, population dynamics, polycentricity, urban land-use evolution, gentrification and urban sprawl. Compared to conventional mathematical tools of spatial simulation such as differential equations, partial differential equations and empirical equations, CA models are relatively simple yet produce results that are quite meaningful and useful to support decision making in a planning context. Although geographical information systems (GIS) are powerful tools to collect, store, manage and analyze spatial data, current GISs have shown considerable weakness and limitation in spatial decision making which are due, in great part, to their lack of sophisticated analytical and spatial modeling tools [5, 6]. Many studies have shown that the integration of geographic information systems (GIS), cellular automata (CA) models, land use allocation models (such as multi-criteria evaluation) and statistical simulation models (such as Markov chains) provides a powerful environment to simulate and predict dynamic phenomena such as urban and rural spatial growth [7].

In this study, the authors present a methodological framework that leverages the suitability-based cellular automata land-use simulation model. The proposed approach involves loose-coupling geographical information systems with Markov chains, multi-criteria evaluation and cellular automata models to model and simulate the rural land-use dynamics using spatial and thematic data sets covering a section of the Lake Chad

Basin, an endorheic basin supporting a population of over twenty million people living in four African countries (Chad, Cameroon, Niger and Nigeria) where the people are among Africa's most chronically vulnerable to food insecurity due to the devastating impact of natural and anthropogenic drivers of ecological transformation in the basin. Our proposed methodology features a workflow-centric, three-step process starting from change quantification (transition model using Markov Chains) through change location (potential model using MCE) to change differentiation (cellular automata). A time-series of multi-scale, multi-resolution and multi-temporal historical satellite imagery and other existing 1:50,000 topographical maps of the study site served as input spatial data sets to determine and delineate the landscape features and the land-use/land-cover trends over the period from 1975 through 1987 to 1999. Bio-physical data (digital elevation model and precipitation data) and accessibility data (distance to roads, distance to water and distance to settlements) served as input suitability spatial factors that were compiled, analyzed and assessed to quantify spatial dependencies using raster-based map algebra and spatial statistical techniques.

1.1 Markov Chains Model

A Markov chain model is defined by a set of states and a set of transitions with associated probabilities where the transitions emanating from a given state define a distribution over the possible next states. The controlling factor in a Markov chain is the transition probability, a conditional probability for the system to undergo transition to a new state, given the current state of the system. One special class of Markov chains that finds wide application in practical simulation problems is the homogeneous Markov chain. A problem can be considered as a homogeneous Markov chain if it has the following properties:

- For each time period, every object in the system is in exactly one of the defined states;
- The objects move from one state to the next according to the transition probabilities which depend only on the current state (previous history is not taken into account);
- The transition probabilities do not change over time.

A homogeneous Markov chain can be represented mathematically as follows (Eqs. (1) and (2)).

$$\mathbf{Q}_{t+1} = \mathbf{Q}_t^{\mathrm{T}}\mathbf{P}^{\mathbf{n}} \tag{1}$$

$$\begin{pmatrix} \mathbf{q}_1 \\ \mathbf{q}_2 \\ \cdots \\ \mathbf{q}_m \end{pmatrix}_{t+1} = \begin{pmatrix} \mathbf{q}_1 \\ \mathbf{q}_2 \\ \cdots \\ \mathbf{q}_m \end{pmatrix}_t^{\mathrm{T}} \begin{pmatrix} \mathbf{p}_{11} & \mathbf{p}_{11} & \cdots & \mathbf{p}_{11} \\ \mathbf{p}_{21} & \mathbf{p}_{22} & \cdots & \mathbf{p}_{2m} \\ \cdots & \cdots & \cdots & \cdots \\ \mathbf{p}_{m1} & \mathbf{p}_{m2} & & \mathbf{p}_{mm} \end{pmatrix}^{\mathbf{n}} \tag{2}$$

where,

n = number of time steps;

m = number of states;

Q_t = vector of initial states at an initial time, t;

Q_{t+1} = vector of states at the next time, $t + 1$;

P = transition probabilities matrix.

A common practical application of the Markovian simulation model is the prediction of a future land-use scenario given a past history of land-use situations. In this analytical situation, the states are represented by the land-use classes (e.g., the classes in a classified satellite image). An example of a Markov transition probability is the probability of one land-use class at an initial time, t changing to another (or remaining in the same) class at a later time, $t + 1$. The crossing of two raster-structured maps representing the terrain situation at two different times is a contingency table (class occupation statistics) of the classes from the two maps. The table is known as the transition cells matrix and can be used to compute the transition probabilities matrix by dividing every entry in a row (class at an initial time) by the total number of cells in that row.

1.2 Multi-criteria Evaluation

Land-use change is often modelled as a function of a selection of socio-economic and bio-physical variables that act as the "driving forces" or factors of land-use change [8]. Driving forces are generally categorized

into three main groups [9]: socio-economic drivers (e.g. population pressure, income levels and agricultural production), bio-physical drivers (e.g. climatic factors such as rainfall, temperature, humidity and topographical variables such as altitude, slope and aspect) and proximate or accessibility factors (e.g. distance to road, distance to settlement and distance to water).

Multi-criteria decision-making (MCDM) or multi-criteria evaluation (MCE) problems involve a set of alternatives that are evaluated on the basis of a set of evaluation criteria [10]. Using MCE, different factors or change drivers can be combined using appropriate weights assigned to the factors. The result of such a combination is a numerical value map representing the land "transition suitability" or "transition potential" values (scores), that describe the potential of cells to undergo transition from a current state (e.g. "forest") to a new state (e.g. "built-up"). A number of methods have been proposed for weighting the factors. Examples include direct weighting, rank-order weighting and analytical hierarchy process (AHP). Of these approaches, AHP has been identified as a weighting strategy that can overcome the problem of weighting bias which are obvious short-comings of the direct and rank-order methods [11]. AHP can be used to determine the relative importance of a set of activities or criteria through a pair-wise comparison of the various factors. The first step of the AHP is to form a hierarchy of objectives, criteria and all other elements involved in the problem. Once the hierarchical structure has been formed, comparison matrices are developed as results of evaluations made by the decision-makers on the intensity of difference in importance, expressed as a rank number on a given numerical scale for each level in the hierarchy. This forms the basis of the final computation of the factor weights. An elaborate description of the MCE process based on the AHP concept can be found in Ref. [10]. In a typical practical application, the factors (input) into the process are spatial factors or factor maps (e.g. aspect map, slope map, distance map, population surface map, etc.), spatial constraints (e.g. a binary map of the exclusion zones such as maps of underground treatment plants, water canal, landfill sites, etc.) and non-spatial constraints. Some MCE modelling methods require that the factors be standardized prior to the computation of the final transition suitability (potential) map [12].

1.3 Cellular Automata

Cellular Automata (CA) are dynamic models that can be employed to simulate the evolution or dynamics of a wide variety of natural and human systems. They are processing algorithms that were originally conceived by Ulam and Von Neumann in the 1940s to study the behavior of complex systems [13]. CA models present a powerful simulation environment represented by a grid of space (raster), in which a set of transition rules determine the site attribute of each given cell taking into account the attributes of cells in its vicinities. These models have been very successful in view of their operationality, simplicity and ability to embody both logic and mathematics-based transition rules, thus enabling complex global patterns to emerge directly from the application of simple local rules. A cellular automaton system consists of a regular grid of cells, each of which can be in one of a finite number of k possible states, updated synchronously in discrete time steps according to a local, identical interaction (transition) rule. The state of a cell is determined by the previous states of a surrounding neighborhood of cells. The types of spatial problems that can be approached using CA models include spatially complex systems (e.g., landscape processes), discrete entity modeling in space and time (e.g., ecological systems, population dynamics) and emergent phenomena (e.g., evolution, earthquakes). From the application perspective, CA are dynamic models that inherently integrates spatial and temporal dimension.

CA is composed of a quadruple of elements as defined in Eq. (3) [14].

$$CA = \{X, S, N, R\} \quad (3)$$

where,

CA = cellular automaton;

X = CA cell space;

S = CA states;

N = CA cell neighbourhood;

R = CA transition rule.

Cell space: The cell space is composed of individual cells. Although these cells may be in any geometric shape, most CA adopts regular grids to represent such space, which makes CA very similar to the cellular structure of raster GIS.

Cell states: The states of each cell may represent any spatial variable, e.g., the various land-use types. The state transition of a CA is defined by Eq. (4):

$$_{t+1}\mathbf{S}_{i,j} = \mathbf{f}((_t\mathbf{S}_{i,j}),(_t\mathbf{N}_{i,j}),(_t\mathbf{R}_{i,j})) \quad (4)$$

where,

$_{t+1}S_{i,j}$ = new (next) state of a cell, $C_{i,j}$ at time t+1;

$_tS_{i,j}$ = initial state of a cell, $C_{i,j}$ at time t;

$_tN_{i,j}$ = neighbourhood of a cell, $C_{i,j}$ at time t;

$_tR_{i,j}$ = transition rule applied to cell, $C_{i,j}$ at time t.

Transition rules: Transition rules guide and control the dynamic evolution of CA. In classical CA, transition rules are deterministic and unchanged during evolution. In several recent studies, however, they are modified into stochastic and fuzzy logic controlled methods [14].

Neighbourhood: This is defined by the local neighbours of a cell. In a two-dimensional cellular automata model there are two common types of neighbourhood: the Von Neumann neighbourhood with four neighbouring cells and the Moore neighbourhood with eight neighbours (see Fig. 1).

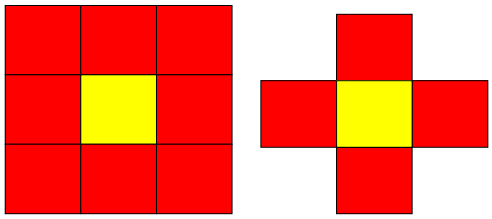

(a) (b)

Fig. 1 3 × 3 neighbourhood Kernels showing: (a) Moore neighbourhood and (b) Von Neumann neighbourhood.

The future state of a cell in a CA is dependent on its current state, neighborhood states, and transition rules which are setup and fine-tuned using transition suitability or potential scores of individual cells. Iterative local interactions between cells within the neighborhood finally produce the global pattern.

2. Study Site

The site for this study is a section of the Lake Chad Basin, an endorheic basin located approximately between latitudes 12°N and 14°30′N and longitudes 13°E and 15°30′E. The basin is shared by four West African countries namely, Chad, Cameron, Nigeria and Niger and supports a population of over twenty million people. The Lake basin comprises five bio-climatic zones, namely, Saharan, sahelo-saharan, sahelo-sudanian, dudano-sahelian and sudano-guinea ecological zones. The south-west humid Atlantic (monsoon) and the north-east Egyptian hot and dry (harmattan) currents influence the climate and consequently the ecological zonation of the basin. The sudano-guinean climate in the south for example has annual rainfall of over 950 mm, a rainy season of six to seven months (May-November) with an average annual temperature at Sarh of 28 °C (absolute minimum 10 °C, absolute maximum 45 °C) and annual Piche-recorded evaporation of 3222 mm in 1961 [15]. The topography of the lake basin can be described as generally flat with a few shallow depressions and a few widely scattered elevated spots. In terms of hydrogeology, the basin lies in a tectonic zone with an extensive sedimentary basin where depositional events, resulting in the formation of four aquifers, had taken place in tertiary and quaternary times [16, 17]. The soil characteristics of the Chad basin region are Ferruginous Tropical and undifferentiated semi-arid brown soils. These cover about two-fifths of the basin while the remaining 60 percent is covered by a zonal vertisols, regosols and mixtures of alluvial and vertisols characterized by a high shrink-swell potential. The Nigerian section of the basin has been rated as soil

having about 90 percent potentiality of medium to high fertility. The predominant vegetation of the basin is comprised of the woodland and pseudo-steppe types populated with trees and shrubs. Fig. 2 shows a map of the study site depicting a section of Lake Chad Basin chosen for this study.

3. Data, Materials and Methods

3.1 Data Sources

The simulation of rural land-use dynamics undertaken in this study for the chosen site was intended to statistically and spatially associate future land-use scenarios with historical growth patterns in the study area by employing the site attributes (bio-physical data) covering the area. Consequently, the following spatial data types were obtained: a set of satellite image data acquired at three different dates; topographical maps; digital elevation data; and climatic data. A set of three Landsat image scenes acquired at three different dates (1975, 1987 and 1999) were downloaded from the Global Land Cover Facility (GLCF) digital image archive [19]. The 1975 Landsat TM image was obtained in the mosaicked format with a spatial resolution of 30 m. The 1987 Landsat TM came with a spatial resolution of 30 m while the 1999 Landsat ETM+ image had a spatial resolution of 28.5 m. Scanned copies of the 1:50,000 topographical maps covering the study site were obtained from the Office of the Surveyor-General of the Federation (OSGOF) of Nigeria. An appropriate image tile of the Advanced Spaceborne Thermal Emission and Reflection Radiometer (ASTER) GDEM was downloaded from National Aeronautics and Space Administration (NASA) Reverb data [20]. Similarly, a tile of Global Climate Database of the Consultative Group for International Agriculture Research-Consortium for Spatial Information (CGIAR-CSI) rainfall data covering the study site was downloaded from the climate database [21]. Table 1 presents a summary of the types, sources, scale/spatial resolution and acquisition dates of the required data sets while Fig. 3 shows colour composites of the acquired 1975, 1987 and 1999 Landsat images.

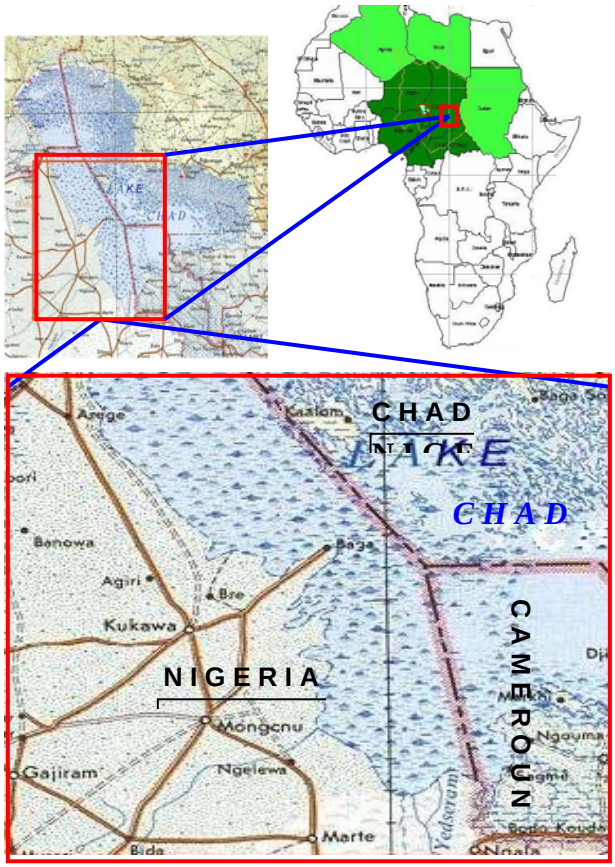

Fig. 2 Map of study site showing a section of Lake Chad Basin (Source: Ref. [18]).

3.2 Materials

Although several off-the-shelf GIS and digital image processing software packages exist and have been successfully used by several researchers to implement CA-based spatial simulations (see Ref. [1]), such tools were not available to us during the course of this study. However, an open-source digital image processing and GIS package, Integrated Land and Water Information System [12] was found adequate for the execution of most of the data processing, conversion, integration and presentation tasks. Special tasks and functionalities required for the simulation which are not supported in the ILWIS software were implemented using in-house programs developed in Visual Basic 6.0 environment.

Table 1 Spatial data sets employed in the study.

Data	Source	Scale/resolution	Date
Landsat TM	GLCF	30 m	1975
Landsat TM	GLCF	30 m	1987
Landsat ETM+	GLCF	28.5 m	1999
Topographical map	OSGOF	1:50,000	1965
ASTER GDEM	ASTER	30 m	2009
CGIAR-CRU rainfall	CGIAR-CRU	0.5°	1999

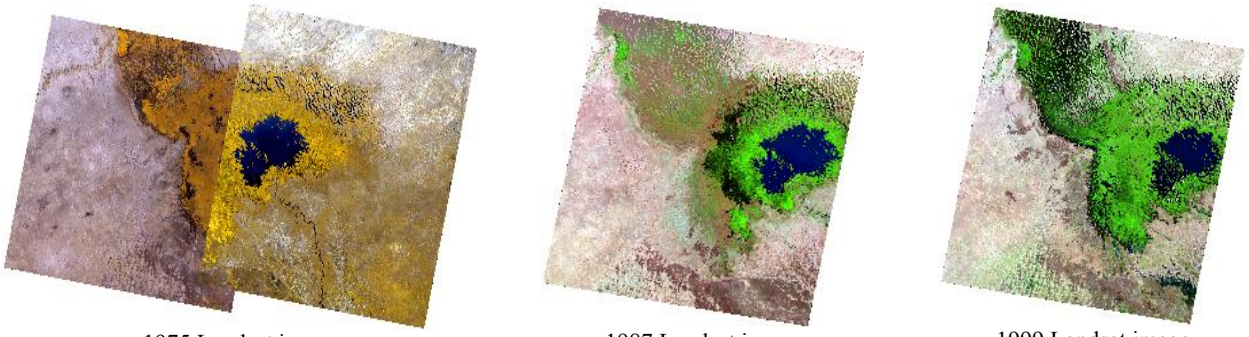

1975 Landsat image 1987 Landsat image 1999 Landsat image

Fig. 3 Colour composites of source Landsat images of 1975, 1987 and 1999.

3.3 Methodology

3.3.1 Data Preparation, Conversion and Processing

Our proposed framework for simulating rural land-use dynamics requires five input maps as summarized in Table 2.

The first step in our methodological approach was the pre-processing of input maps and tables for the simulation. All the required data sets were first imported into the ILWIS environment and converted into ILWIS format. The CGIAR-CRU Rainfall data (point raster format) was then interpolated using the Inverse Distance Weighted (IDW) method and re-sampled to obtain a 30-m resolution surface map. All the three satellite images, including the scanned topographical maps, the ASTER-GDEM and the CGIAR-CRU rainfall surface map, were then geo-referenced to the UTM (Zone 33) projection on WGS84 Ellipsoid using ground control (tie-points) read off from the topographical maps. The required slope and aspect maps were then derived from the ASTER-GDEM (altitude) map using raster map calculation. Marked differences in spectral characteristics due probably to disparities in image acquisition conditions were observed on the 1975 (mosaicked) source image. Since this could lead to erroneous classification results, this image was first unglued to obtain its component parts. In the study area, seven land-use classes (Road, Settlement, Water, Wetland, Openland, Farm and Forest) were identified and considered as candidate "states" for the simulation.

Table 2 Input maps for CA-based simulation.

Input map	Description
Initial configuration	Initial (seed) scenario for the simulation
Transition suitability map	Transition potential values for each land-use class
Suitability threshold map	Suitability cut-off values for each land-use class
Predominant count map	Count of the predominant class within the neighbourhood of each cell of the original (initial configuration) map
Predominant class map	Class with the predominant count within the neighbourhood of each cell of the original (initial configuration) map

However, all the source images were classified into only five land-use classes (Water, Wetland, Openland, Farm and Forest). The Road and Settlement classes were omitted from the classification since they showed very similar spectral characteristics with the Openland class. The separate components of the 1975 image were first classified in the ILWIS environment using the maximum likelihood classifier and finally glued back together to obtain a seamless image. The same digital classification parameters were then applied to classify the 1987 and the 1999 images. To include the Road and Settlement classes, the two feature types were extracted from the topographical maps by on-screen digitizing and overlaid on each of the three original images. The corresponding polygons (Settlement class) and segments (Road class) were then updated to reflect the situation at each period. Each of the Road and Settlement layers so delineated were then rasterized and merged into the corresponding classified image using raster map calculation function available in ILWIS. Finally, a spatial constraint map layer was created by digitizing the Water Canal features from the topographical maps. Similarly, three accessibility maps (distance to road, distance to settlement and distance to water) were generated from the road, settlement and water layers using the distance calculation function in ILWIS. An extract of the defined study area was thereafter made from each of the resulting images and stored for further analysis. The final 1975, 1987 and 1999 classified images are shown in Fig. 4.

In this study, the authors adopted the classified 1999 image (latest image) as the initial (seed) configuration for the CA simulation. Based on this classified image, the neighbourhood predominant count map and the neighbourhood predominant class maps were generated by applying the neighbourhood map calculation functionalities supported in the ILWIS software based on the Moore neighbourhood (Fig. 1a). To obtain the transition cells matrices, two successive classified images were crossed, giving the class occupation statistics of the two image pairs. The 1975-1987 and 1987-1999 transition cells matrices so obtained were then employed to compute the corresponding transition probabilities matrices as described in Section 1.1. Using the method described in Ref. [22], a homogeneous transition matrix representing the general trend of land-use evolution over the period between 1975 and 1999 was computed based on the two separate transition matrices. The homogeneous transition matrix and the class populations (initial states vector) from the seed image constituted input variables for the computation of the transition model.

The transition (quantification of land-use changes) model for the simulation was then executed to obtain simulated rates of change corresponding to two future scenarios (2011 and 2023). Adopting the latest period (1999) as the initial (seed) period, the homogeneous Markov chain model (Eq. (2), Section 1.1) was applied (substituting the homogeneous transition matrix for P and the 1999 class population values for Q) to compute simulated transition rates (cells) for 2011 (n = 1 or first time step) and 2023 (n = 2 or second time step). The results obtained from this operation are as

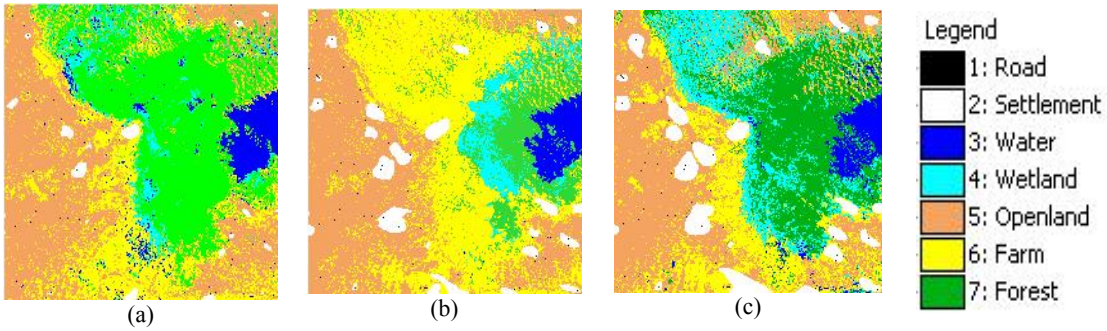

(a) (b) (c)

Fig. 4 Classified images of: (a) 1975; (b) 1987 and (c) 1999.

summarized in Tables 3(a), 3(b) and 3(c). From Tables 3(b) and 3(c), the suitability threshold map was generated by interpolating the values in these tables (column F) from the cumulative histograms of the individual classes for the two scenarios (Table 4). This operation was performed using an in-house program developed in Visual Basic 6.0. A composite suitability threshold map was finally generated by assigning the computed threshold values to each of the land-use classes.

The next step in the simulation process was the computation of the potential model (using MCE) to generate the transition suitability (potential) maps. In this study, seven spatial factors—(altitude, slope, rainfall, distance to road, distance to settlement and distance to water and one spatial constraint (water canal), were considered to affect the suitability of cells for conversion into other land-use classes. Socio-economic factors such as population density and agricultural productivity were not available during the course of this study. For each of the available factors, a factor map was prepared. This process was effected in ILWIS by first creating a factor group for each land-use class and then populating the group with the maps corresponding to each of the factors. This was followed by a process of standardization of each map considering the overall goal of the evaluation in relation to the contribution of each factor towards the

Table 3 Simulation statistics: (a) class populations for seed and simulated configurations; (b) gains and losses for 1999-2011 simulation; (c) gains and losses for 1999-2023 simulation.

(a)

LU classes	Class populations		
	1999	2011	2023
Road	40596	45216	50465
Settlement	1661531	2186508	2706862
Water	984230	900545	825165
Wetland	2977357	1900899	2018867
Openland	7191009	6584558	6541046
Farm	4202185	6196237	6138675
Forest	5339142	4582088	4114970

(b)

Class	A	B	C	D	E	F	G
Road	40596	5401	781	4620.1	13.3	1 .9	11.4
Settlement	1661538	599371	74394	524976.4	36.1	4.5	31.6
Water	984234	189062	272747	-83685.2	19.2	27.7	-8.5
Wetland	2977370	1551940	2628398	-1076458.1	52.1	88.3	-36.2
Openland	7191041	1056422	1662872	-606450.8	14.7	23.1	-8.4
Farm	4202204	4606912	2612860	1994052.0	109.6	62.2	47.5
Forest	5339166	2424867	3181922	-757054.4	45.4	59.6	-14.2

(c)

Class	A	B	C	D	E	F	G
Road	40596	11415	1546	9868.9	28.1	3.8	24.3
Settlement	1661538	1187798	142467	1045331.2	71.5	8.6	62.9
Water	984234	307434	466499	-159065.3	31.2	47.4	-16.2
Wetland	2977370	1587111	2545601	-958490.2	53.3	85.5	-32.2
Openland	7191041	2040933	2690895	-649962.5	28.4	37.4	-9.0
Farm	4202204	4783369	2846879	1936490.2	113.8	67.7	46.1
Forest	5339166	2445938	3670110	-1224172.3	45.8	68.7	-22.9

A = number of cells in the seed map; B = gain in cells between initial and simulated maps; C = loss in cells between initial and simulated maps; D = net gain in cells between initial and simulated maps; E = % gain in cells between initial and simulated maps; F = % loss in cells between initial and simulated maps; G = % net gain in cells between initial and simulated maps.

Table 4 Predicted transition suitability threshold values for 1999-2011 and 1999-2023 simulations.

Land-use class	Suitability threshold value (2011)	Suitability threshold value (2023)
Road	0.916626547	0.912322272
Settlement	0.962713488	0.956168315
Water	0.757331349	0.746932254
Wetland	0.738712870	0.673720590
Openland	0.815529404	0.788445542
Farm	0.787391162	0.777337315
Forest	0.737500963	0.730205614

goal. The factors per group were then weighted using the Analytical Hierarchy Process (AHP) by pair-wise comparison of factors (see Ref. [23] for details). This resulted in specific weights assigned to each factor (see Table 5). The AHP was assessed using the inconsistency ratios and the computed weights were accepted and used in the computation of a composite index map (suitability map) for each factor. Thus seven different suitability maps corresponding to the seven different land-use classes were obtained from the MCE-AHP process. To obtain a single suitability map, all the seven suitability maps were combined using the map calculation functionality in ILWIS. The final transition suitability map was then generated using cell-by-cell multiplication of the composite suitability map and the binary constraint map. This operation assigned a suitability value of zero (unsuitable) to all cells corresponding to the water canal feature.

3.3.2 Cellular Automata Simulation Runs

In keeping with the goal of simulating the rural land-use dynamics for our study area, CA-based transition rules (algorithms) were implemented in an ILWIS-based script. In designing the CA transition rule, the Moore neighbourhood kernel (see Section 1.3) was adopted with a kernel threshold of 3. A cell would therefore undergo state transition to the state of the predominant cell in its 8-cell neighbourhood if its transition suitability value is greater than zero and if it is not "Settlement" or "Road" and if its transition suitability value is greater than the suitability threshold value and if the count of the predominant cell is greater than or equal to the neighbourhood kernel threshold value of 3. It is to be noted that several other constraints can be integrated into the transition rule to achieve some set configuration. Algorithm 1 shows a simple basic-like CA-based transition algorithm developed for the simulation. The script was designed to reference the five raster-structured maps generated in the previous sub-section as input maps to compute final (simulated) raster maps corresponding to the 1999-2011 and 1999-2023 scenarios based on neighbourhood map calculation. Fig. 5 shows the resulting simulated maps for the two proposed scenarios.

Table 5 Multi-criteria evaluation factor weights for different land-use classes computed based on analytical hierarchy process (AHP).

Factors	Land-use classes						
	Road	Settlement	Water	Wetland	Openland	Farm	Forest
Altitude	0.140	0.036	0.045	0.116	0.053	0.032	0.047
Slope	0.071	0.073	0.070	0.089	0.053	0.049	0.053
Aspect	0.071	0.085	0.029	0.054	0.053	0.028	0.026
Rainfall	0.045	0.025	0.315	0.325	0.333	0.335	0.431
Distance to road	0.316	0.278	0.096	0.046	0.109	0.154	0.115
Distance to settlement	0.231	0.158	0.131	0.044	0.109	0.116	0.192
Distance to water	0.127	0.346	0.315	0.325	0.291	0.287	0.134
Total weight	1.000	1.000	1.000	1.000	1.000	1.000	1.000
Inconsistency ratio	0.099	0.089	0.090	0.049	0.059	0.099	0.090

```
------------------------------------------------------------------------
If (Suitability_Map = 0) Then
   Simulated_Map = Initial_Map; 'No change in cell state
Else
   If ((Initial_Map = "Settlement") Or (Initial_Map =
     "Road")) Then
     Simulated_Map = Initial_Map; 'No change in cell state
   Else
      If ((Suitability_Map >= Suitability_Threshold_Map)
        And (Predominant_Count >= 3)) Then
        Simulated_Map = Predominant_Class; ' Update cell
         state
      Else
        Simulated_Map = Initial_Map; 'No change in cell
         state
      End if
   End if
End if
------------------------------------------------------------------------
```

Algorithm 1 Basic-like CA-based transition rule for the simulation.

3.3.3 Simulation Evaluation

In order to determine the degree of reliability of the simulation results, a numerical evaluation was executed using the historical image data sets for the three periods (1975, 1987 and 1999). This task was done by simulating transition rates for 1987 and 1999 using the 1975 and 1987 class populations respectively based on Markov Chains prediction model. For each simulation scenario, the accuracy in the estimation of each land-use class was computed using the following formula:

$$\text{Accuracy}(\%) = 100\left(1 - \text{abs}\left(\frac{\text{Simulated Value} - \text{Real Value}}{\text{Real Value}}\right)\right)$$

The results obtained for the two scenarios are as presented in Table 6.

4. Results and Discussion

The quantitative results of the integrated spatial simulation of rural land-use dynamics undertaken in this study are presented in Tables 3 and 4 while its graphical (image) outputs are presented in Fig. 5. As shown in Tables 3(b) and 3(c), Water, Wetland, Openland and Forest classes were predicted to register net losses of 8.5%, 36.2%, 8.4% and 14.2% respectively for the 2011 scenario and 16.2%, 32.2%, 9.0% and 22.9% respectively for the 2023 scenario, while Road, Settlement and Farm classes were predicted to register net gains of 11.4%, 31.6%, and 47.5% respectively for the 2011 scenario and 24.3%, 62.9% and 46.1% respectively for the 2023 scenario. As can be discerned from Table 6, the accuracies of the simulation of the various land-use change rates are

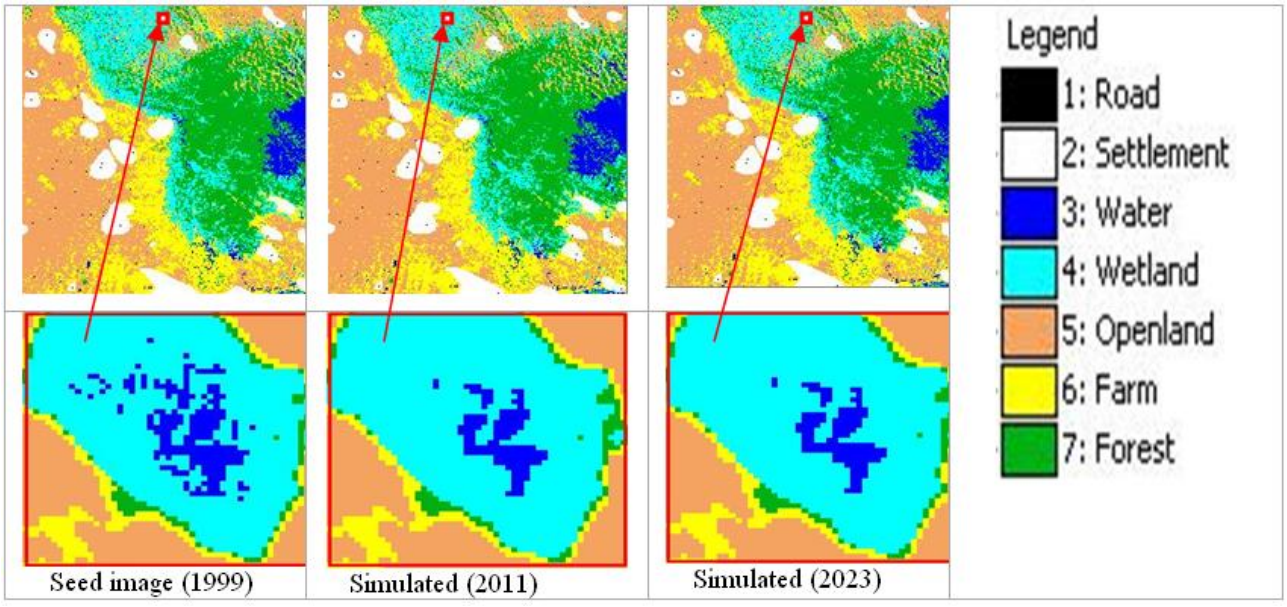

Fig. 5 Seed image (1999) and simulated images (2011 and 2023).

Table 6 Simulation evaluation results.

Land-use class	Simulation for 1987			Simulation for 1999		
	Real	Predicted	Accuracy (%)	Real	Predicted	Accuracy (%)
Road	38378	35177	91.7	40596	39781	98.0
Settlement	1135212	941912	83.0	1661531	1564405	94.2
Water	882703	1074995	78.2	984230	957563	97.3
Wetland	1148271	2051885	21.3	2977357	2109228	70.8
Openland	8016597	7109876	88.7	7191009	7016688	97.6
Farm	8561286	6642613	77.6	4202185	6429666	47.0
Forest	2613603	4539592	26.3	5339142	4278720	80.1

better for the 1999 scenario (long-tern projection) than that for the 1987 scenario (short-tern projection). This situation needs to be further investigated.

From the initial and simulated images presented in Fig. 5, the morphological changes in the land-use classes between the original image and its simulated versions are clearly visible.

5. Conclusion and Recommendations

An integrated methodological approach featuring the coupling of GIS with Markovian, MCE and CA models for modelling and simulating the spatio-temporal dynamics in a rapidly changing ecosystem (the Lake Chad Basin) was presented in this study. The proposed integrated model was successfully used to model, analyze and construct future land-use scenarios based on empirical, ground-truth spatial data sets acquired over a period of twenty-four years (1975-1999). The results of the simulation analysis indicate that the Lake Chad ecosystem is steadily undergoing land-use/land-cover changes. In particular, the study reveals that the water stock of the lake is rapidly shrinking.

This study was conducted on only a section of the basin. To perform a more comprehensive analysis of the causes and consequences of the land-use dynamics in the basin, the study area needs to be extended to cover the entire basin. Socio-economic factors that were not available for the determination of the transition potential values also need to be integrated in future studies to enhance the realism of the simulation.

The results obtained from this study demonstrate that integrated rural land-use scenario building and analysis relying on the CA-based land-use simulation model can support land-use planning and policy for sustainable land development. However, issues concerning simulation evaluation, calibration and validation need to be further considered and investigated.

References

[1] T. Houet, L. Hubert-Moy, Modelling and projecting land-use and land-cover changes with a cellular automaton in considering landscape trajectories: An improvement for simulation of plausible future states, in: EARSeL eProceedings, Vol. 5, 2006, pp. 63-76.

[2] C. Kamusoko, M. Aniya, B. Adi, M. Manjoro, Rural sustainability under threat in Zimbabwe—Simulation of future land use/cover changes in the Bindura district based on the Markov-cellular automata model, Apply Geography 29 (2009) 435-447.

[3] R. Costanza, M. Ruth, Using dynamic modelling to scope environmental problems and build consensus, Environmental Management 22 (1998) 183-195.

[4] M. Batty, H. Couclelis, M. Eichen, Urban systems as cellular automata, Environment and Planning B: Planning and Design 24 (1997) 159-164.

[5] J. Malczewski, A GIS-based approach to multiple criteria group decision-making, International Journal of Geographic Information Systems 10 (1996) 955-971.

[6] S. Park, D.F. Wagner, Incorporating cellular automata simulators as analytical engines in GIS, Transactions in GIS 2 (1997) 213-231.

[7] K.C. Clarke, S. Hoppen, L. Gaydos, A self-modifying cellular automaton model of historical urbanization in the San Francisco Bay area, Environment and Planning B: Planning and Design 24 (1997) 247-261.

[8] E. Lambin, H.J. Geist, E. Ellis, Causes of land-use and land-cover change [Online], http://www.eoearth.org/article/Causes_of_land-use_and_l

and-cover_change.

[9] E.F. Lambin, B.L. Turner, H. Geist, S. Agbola, A. Angelsen, The causes of land-use and land-cover change: Moving beyond the myths, Global Environmental Change 11 (2001) 261-69.

[10] N. Jacoba, R. Krishnan, R. Prasada, J. Saibaba, Spatial and dynamic modeling techniques for land use change dynamics study, The International Archives of the Photogrammetry, Remote Sensing and Spatial Information Sciences 37 (2008) 37-43.

[11] L. Deekshatulu, R. Krishnan, J. Novaline, Spatial analysis and modelling techniques—A review, in: Proceedings of Geoinformatics-Beyond 2000 Conference, Indian Institute of Remote Sensing Dehra Dun, India, 1999, pp. 268-275.

[12] ILWIS 3.0 Academic Users' Manual, International Institute for Aerospace Survey and Earth Sciences (ITC), The Netherlands, 2007, p. 530.

[13] M.A. Harrison, 4/67-1R Theory of Self-Reproducing Automata, 1966, in: John von Neumann, Arthur W. Burks (Eds.), University of Illinois Press, American Documentation, 1967, p. 254.

[14] F. Wu, C.J. Webster, Simulation of land development through the integration of cellular automata and multi-criteria evaluation, Environment and Planning B: Planning and Design 25 (1998) 103-126.

[15] S. Vassolo, The acquifer recharge and storage systems to halt the high level of evapotranspiration, in: FAOWATER Seminar Proceedings on Adaptive Water Management in the Lake Chad Basin, Stockholm, Aug. 16-22, 2009, pp. 30-43.

[16] The Wood Explorer, Country data on Lake Chad Basin Wensite [Online], http://www.thewoodexplorer.com/countrydata/Chad/home.html.

[17] H.K. Ayouba, The application of climate adaptation systems and improvement of predictability systems in the lake chad basin, in: FAOWATER Seminar Proceedings on Adaptive Water Management in the Lake Chad Basin, Stockholm, Aug. 16-22, 2009, pp. 19-28.

[18] Wikipedia, Published 1973 topographical map extract of Lake Chad Basin, [Online], http://en.wikipedia.org/wiki/Lake_Chad.

[19] Global Land Cover Facility (GLCF), Landsat TM/ETM+ image of 1975, 1987 and 1999 [Online], http://www.glcf.com.

[20] National Aeronautics and Space Administration (NASA), ASTER 30-m GDEM data [Online], http://reverb.echo.nasa.gov/reverb/.

[21] Consultative Group for International Agriculture Research - Consortium for Spatial Information (CGIAR-CSI), Global Climate data, [Online], http://cru.csi.cgiar.org.

[22] A. Berchtold, Chaînes de Markov et modèles de transition: Application, aux sciences sociales, Hermes, 1998, p. 284.

[23] T.L. Saaty, Relative measurement and its generalization in decision making: Why Pairwise Comparisons are Central in Mathematics for the Measurement of Intangible Factors-The Analytic Hierarchy/Network Process, Rev. R. Acad. Cien. Serie. A. Mat. 102 (2008) 251-318.